

DOI: 10.35595/2414-9179-2020-1-26-547-560

**Bobomurat J. Ahmedov¹, Bahadir S. Mirzaev¹, Farmon M. Mamatov¹,
Dadakhon A. Khodzhaev¹, Mukhiddin K. Julliev¹**

INTEGRATING OF GIS AND GPS FOR IONOSPHERIC PERTURBATIONS IN D- AND F-LAYERS USING VLF RECEIVER

ABSTRACT

Regular monitoring of the D- and F-layers of ionosphere over Central Asia territory is being performed on the permanent basis starting year 2008 when one Very Low Frequency (VLF) receiver and two SuperSID receivers were provided to Uzbekistan IHY cite by Stanford University. The results obtained at Tashkent IHY (International Heliophysical Year) station are applied to earthquake electromagnetic precursors, lightning, and Solar flares and to ionospheric disturbances originating from gamma ray flares of Soft Gamma-Ray Repeaters.

Regular monitoring of the D-layer of ionosphere over Central Asia territory has been performed on the permanent basis. Several Solar events are observed and the analysis has shown that there is simultaneous correlation between the times of change of amplitude of the waves and the Solar flares. Features of the lightning discharge generated by radio atmospheric are studied and its effectiveness in D-region ionosphere diagnostics is examined.

We have mainly analyzed GPS derived TEC disturbances from two GPS stations located in Tashkent and Kitab, for possible earthquake ionospheric precursors. The solar and geomagnetic conditions were quiet during occurrence of the selected more than 30 earthquakes. We produced TEC time series over both sites and apply them to detect anomalous TEC signals preceding or accompanying the earthquakes. The results show anomalous enhancements which are examined in the earthquakes.

KEYWORDS: GPS, ionosphere, total electron content (TEC)

INTRODUCTION

The ionizing action of the radiation of Sun on the upper atmosphere produces free electrons. Above about 60 km the number of these free electrons is sufficient to affect the propagation of electromagnetic waves. This “ionized” region of the atmosphere is a plasma and is referred to as the ionosphere. Rishbeth and Garriott in year 1969 have divided the ionosphere in to several layers. The lowest **D layer** varies from 60 to 90 km with the electron concentration 10^1 – 10^4 per cm^3 . D layer ionization is a function of the solar flow. The ions are formed by the ionization of atmospheric neutrals by X-ray radiation and solar Lyman α radiation. This region vanishes at night due to the combination of the ions and electrons. High-frequency (HF) radio waves are not reflected by this region, the main impact of which is absorption of HF radio waves. **E layer** is from 90 to 150 km with the electron concentration 10^5 per cm^3 . Similarly, to the D layer, the E layer shows a diurnal behavior with a maximum of ionization at local noon. In this region, ions consist primarily of O_2^+ produced by the absorption of solar radiation, and NO^+ formed by charge transfer collisions with other ions ionized by coronal X-rays. In auroral region, solar particle precipitation can produce radio scintillation effects in the E layer. The upper **F layer** is from 120 to 800 km with the electron concentration 10^5 per cm^3 . This layer is formed by ionization

¹ Tashkent Institute of Irrigation and Agricultural Mechanization Engineers, Kori Niyoziy str., 39, 100000, Tashkent, Uzbekistan; e-mail: bahadir.mirzaev@bk.ru

of atomic oxygen by Lyman emissions and emissions from He and is the most important part of the ionosphere in terms of HF communications.

The major source of electromagnetic energy in the lower atmosphere is the lightning discharges radiating electromagnetic waves that are the strongest in the VLF frequency range. A number of naval transmitters also operate in the VLF frequency range. The conductivity increases exponentially with height in the lower and middle atmosphere and causes attenuation and dispersion of the low-frequency waves. At radio frequencies, the lower and middle atmosphere behaves like a vacuum and due to this reason low-frequency waves could control the electrodynamics of the lower and middle atmosphere. Sub-ionospherically propagating VLF waves are uniquely suited for the investigation of the nighttime D-region, also known as the 'ignorosphere' (40–100 km altitudes) so named due to the difficulty of making systematic measurements [Tojiev *et al.*, 2014] because it is too low for satellites to complete an orbit (due to high atmospheric drag) and too high for even the largest balloons (~ 30 km) and even the highly specialized extremely high altitude aircraft (~20 km) and is thus only accessible by rockets in the course of a single brief traverse through the region.

Global Positioning System (GPS) is space-based radio navigation system operated by the United States Government. GPS is a satellite-based navigation system made up of a network of 24 satellites, which are distributed in six orbital planes around the globe at an altitude of about 20162.61 km. The total signal for each satellite in GPS comprises of two transmission signals: the L1 signal having carrier frequency of 1575.42 MHz and the L2 signal of 1227.60 MHz and the ionosphere represents the largest source of positioning error for GPS users. In addition, the effects of the ionosphere can cause range-rate errors for GPS satellite users who require high accuracy measurements. The parameter of the ionosphere that affects the radio signals that propagate through this layer is known as Total Electron Content (TEC). TEC is an integral of electron density along the path between the GPS satellite and the receiver.

MATERIALS AND METHODS OF RESEARCHES

I. Ionospheric study in D-layer over Central Asia

Central Asian research program is designed to address outstanding scientific questions concerning transient and localized variations of the nighttime lower ionosphere (< 90 km). The Very Low Frequency (VLF) remote sensing measurements will be conducted with Stanford-built equipment in Tashkent, as shown in fig.1.

The conducting Earth is surrounded by comparatively non-conducting atmosphere of thickness 60–80 km. The layer above it is the ionosphere extending up to ~ 1 000 km which is the uppermost part of the atmosphere, distinguished because it is ionized by solar ultraviolet and X-Ray wavelengths radiation. At heights of above 80 km the atmosphere is so thin that free electrons can exist for substantial periods of time before recombining with an ion. The number of these free electrons is sufficient to affect radio wave propagation. The amount of ionization in the ionosphere varies greatly with the amount of radiation received from the Sun depending on diurnal, seasonal effects, the sunspot cycle, and latitude. There are also mechanisms that disturb the ionosphere and decrease the ionization.

Fig. 2 shows schematically the role of the ionosphere in radio wave propagation. The D-region of ionosphere is the innermost layer (from 50 km to 90 km above the surface of the Earth) where ionization is due to Lyman series-alpha hydrogen radiation. In addition, when the Sun is active with 50 or more sunspots, hard X-rays (wavelength < 1 nm) ionize the air. During the night cosmic rays produce a residual amount of ionization. Recombination is high in the D-region thus the net ionization effect is very low and as a result high-frequency radio waves are not reflected by the D layer. The frequency of collision between electrons and other particles in this region during the day is about 10 MHz. The D layer is mainly responsible for absorption of radio waves, particularly at 10 MHz and below, with progressively smaller absorption as the frequency gets

higher. The absorption is small at night and greatest about midday. The layer reduces greatly after sunset, but remains due to galactic cosmic rays.

The major source of electromagnetic energy in the lower atmosphere is the lightning discharges radiating electromagnetic waves that are strongest in the VLF frequency range. A number of naval transmitters also operate in the VLF frequency range. The conductivity increases exponentially with height in the lower and middle atmosphere and causes attenuation and dispersion of the low-frequency waves. At radio frequencies, the lower and middle atmosphere behaves like a vacuum and due to this reason low-frequency waves could control the electrodynamics of the lower and middle atmosphere.

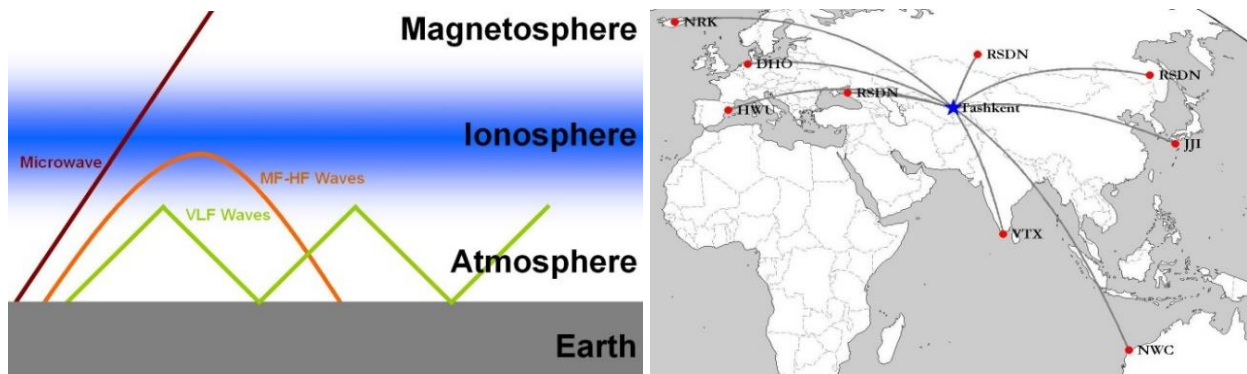


Fig. 1. Left panel: The configuration of VLF paths observed at Tashkent. Amplitudes/phases of signals arriving over great-circle paths from several VLF transmitters located in Europe, Asia, Australia and Russia will all be measured with high time resolution (<10 ms), thus allowing the detection of localized ionospheric disturbances over the Central Asia.

Right panel: The effect of the ionized boundary where the Sun's radiation hits an increasingly less dense atmosphere is to reflect waves of VLF frequencies. Since the Earth also reflects VLF waves, they can be efficiently guided to large distances in the so-called Earth-ionosphere waveguide

Subionospherically propagating VLF waves are uniquely suited for the investigation of the nighttime D-region, also known as the 'ignorosphere' (40–100 km altitudes) so named due to the difficulty of making systematic measurements because it is too low for satellites to complete an orbit (due to high atmospheric drag) and too high for even the largest balloons (~30 km) and even the highly specialized extremely high altitude aircraft (~20 km) and is thus only accessible by rockets in the course of a single brief traverse through the region. Unfortunately, such measurements do not allow the systematic study of variability of the region and is specifically unsuited for the localized and highly transient type of lightning-induced disturbances that are the subject of our proposed study.

Radio methods aimed at measurement of total electron content (TEC) (for example using tomographic techniques using GPS or other signals) are similarly not useful, since these measurements are dominated by the much higher electron densities in the E and F regions. Optical remote sensing can in principle be used, but only the most energetic events, such as the luminous discharges of high altitude known as 'sprites.' The bulk of ionospheric disturbances produced by lightning discharges, specifically the so-called Early/fast events and lightning-induced electron precipitation effects which are the subjects of the proposed study, do not exhibit detectable optical signatures.

Subionospheric VLF measurements are particularly responsive to the study of this altitude range due to the fact that the nighttime reflection height is in the vicinity of ~85 km altitude. Measurements of the amplitude and phase of VLF signals propagating in the earth-ionosphere waveguide have long been used effectively for remote sensing of the ionosphere.

Two different primary types of subionospheric Very Low Frequency (VLF) signatures have been identified resulting from lightning activity, namely (i) the so-called Early/fast VLF conductivity changes in which the subionospheric VLF signal amplitude/phase changes within <20 ms of the causative lightning flash, indicating an immediate effect of the lightning discharge in the overlying lower ionosphere, and (ii) VLF signatures of lightning-induced electron precipitation (LEP) events, in which the subionospheric VLF signal/amplitude changes after an onset delay of ~1 sec with respect to the causative lightning flash, consistent with the finite wave and particle travel times respectively to/from the regions of maximum cyclotron resonant pitch angle scattering of the energetic (>100 keV) radiation belt particles which causes them to precipitate into the lower ionosphere.

VLF waves transmitted from ground-based transmitters in the frequency range of 10–30 kHz are used for navigation, radio communications and ionospheric/magnetospheric investigations. VLF waves are efficiently reflected by the D-region of the ionosphere, and can therefore be guided to global distances from sources. On the other hand, the small amount of energy that is absorbed by the ionosphere can propagate in the whistler mode through the magnetospheric plasma, leading to triggering of new waves, ionospheric heating, wave-particle interactions, particle precipitation and wave amplifications. The VLF wave propagating along the geomagnetic field interacts with the counter streaming energetic electron flux, which is effective in the equatorial region when the Doppler-shifted wave frequency seen by the particles is close to the electron gyrofrequency, an effect known as gyroresonance. During this interaction, particles undergo pitch angle scattering, which may lead to precipitation of the particle into the atmosphere. Impulsive radiation from lightning, some of whose energy escapes into the magnetosphere, is known to produce these so-called Lightning-Induced Electron Precipitation (LEP) events.

The Stanford ELF/VLF radio receiver, known as the Atmospheric Weather Electromagnetic System for Observation, Modeling, and Education (or AWESOME) measures natural and manmade signals in the frequency range between 500 Hz and 47 kHz. Data is recorded with two orthogonal air-core wire loop antennae (a photographed example of which is shown in the bottom left of fig.1). Each loop is sensitive to one component of the horizontal magnetic field, enabling directional information to be extracted from the combination. Incoming VLF signals induce voltages in the loop of wire, however because these voltages are extremely small (100s femtovolt to picovolts range), low-noise amplification is required in order to extract these signals. The preamplifier (shown next to the loops in the same figure photograph) performs this function, and is placed outdoors next to the antenna. The signal is then driven across a long cable, to a line receiver box, which is typically indoors next to a computer. The line receiver applies an anti-aliasing filter, and also synchronizes the signal with GPS timing, so that absolute timing accuracy is 100–200 ns. Using a phase-locked loop, the 1 PPS GPS signal is used to generate a 100 kHz sampling signal, which is fed into a PCI card inside the computer which digitizes and stores the data from both antennae. Software developed by Stanford sets the schedule for recording.

Fig. 2 also shows some sample data taken with the AWESOME receiver at Tashkent. The top left panel shows the data in the form of a spectrogram, where the strength of the signal as a function of time is divided into frequency bins and indicated with a color-scale. The vertical lines are short impulsive radiation from lightning strikes, which could be anywhere in the world, and are known as radio atmospherics, or spherics. These spheres propagate efficiently in the Earth-ionosphere waveguide, to global distances (10 Mm or more from the source), and can reveal properties of the originating lightning stroke, and the ionosphere along the propagation path. An example of a sphere is shown in the lower left panel of the fig. 2. Horizontal lines are VLF transmitter signals, originating from all over the world, and used for long-range communication

with submerged submarines. The zoom-in on the top right shows one such transmitter signal, originating from Germany, with the minimum-shift-keying (MSK) modulation signal apparent as up and down frequency shifts. The software written by Stanford determined this MSK pattern, and subtracts out the associated phase shifts in real time, so that a demodulated phase can be extracted and tracked, along with the amplitude of the signal. Because these VLF transmitter signals are guided by the lower ionosphere (being typically reflected between 70 and 85 km during the daytime and nighttime, respectively), they are extremely sensitive to ionospheric disturbances, and are therefore a unique form of ionospheric diagnostics.

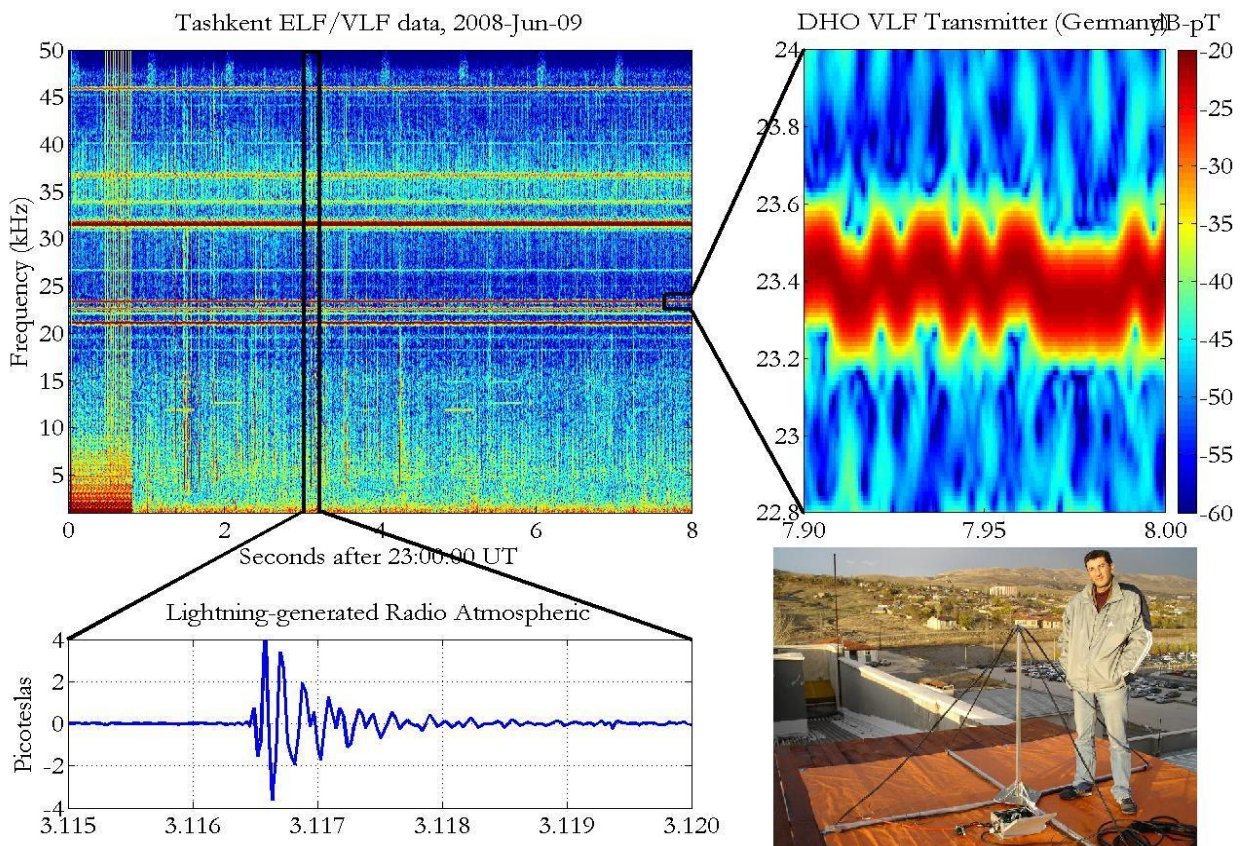


Fig. 2. Data taken with VLF antenna in Tashkent. The top left plot shows a spectrogram, in which the frequency content is divided for individual time bins, and the strength is indicated by the color-scale. The bottom plot shows a time-series zoom-in of a radio atmospheric, i.e., short impulsive radiation from a lightning stroke which may be at global distances. The right plot shows a VLF transmitter signal, in this case originating from Germany, with the MSK communication signal evident by the up and down frequency changes. Since both the radio atmospheric and the VLF transmitter signal rely on the D-region for propagation, the received signals are both extremely sensitive to the various ionospheric disturbances described herein

ELF and VLF transient signals and noise are generated by various natural and artificial phenomena. Those of natural origin include the familiar lightning discharges from thunderstorms associated high-altitude luminous phenomena called sprites, elves and blue-jets, volcanic eruptions, dust storms and tornadoes. Lightning discharges generate transient electromagnetic pulses. The pulse duration of return strokes (responsible for the generation of ELF/VLF waves) is

of the order of 100–200 us, which implies that the maximum spectral energy is in the frequency range 5–10 kHz. The peak pulse amplitude is ~10–100 kA and typical lightning channel length is 5–10 km. Thus, the return stroke is a very powerful generator of ELF/VLF waves in the atmosphere. The wave amplitude is ~1–10 mV.

A small amount of VLF energy is absorbed by the ionosphere into the magnetosphere. The VLF waves propagating in whistler mode along the dipolar geomagnetic field line interact with counter streaming energetic electrons in the equatorial region. During interaction process, energy and pitch angle of interacting electrons decreases leading to their precipitation to the lower atmosphere usually known as whistler-induced electron precipitation/trimipi precipitation/lightning-induced electron precipitation. These precipitated energetic electrons produce additional ionization leading to change in electrical conductivity and hence modify the flow of electric currents and distribution of electric fields.

a. VLF spherics from lightning

The lightning discharge is an electrical breakdown current which may flow from cloud to ground (CG discharge) or within thunderclouds (intra-cloud or IC discharge). The discharge currents generate transient radio pulses termed ‘atmospherics’ or ‘spherics’ which are generated by lightning in the ELF and VLF bands. Spherics are short pulses, typically of 1–10 ms duration, whose vertical electric field can reach values as large as 1 V/m even at ranges of over 1 000 km. They have a significant spectral content over the whole ELF/VLF range and have been used in studies of radio wave propagation in the Earth-ionosphere. Two types of spheric, the ‘slow tail’ and ‘tweek’, have received special attention in radio-wave propagation studies. The slow tail spheric has been used mainly in the studies of ELF propagation whereas the tweek spheric has been used to study nocturnal VLF and upper ELF-band propagation. Tweeks are referred to as echo-type waveforms and simple ray theory analyses could be used to model their propagation between the Earth and the ionosphere.

Sprites (or ‘red sprites’), an example of which is shown to the left, are extended red luminous columns which can be observed at night-using low-light television (LLTV) cameras. They appear as clusters of short-lived (~50 ms) pinkish-red luminous columns, stretching from ~30 to ~90 km altitude. They are generally <1 km wide and occur above active thunderstorms, especially so-called ‘mesoscale convective systems.’

b. Climate change connection to thunderstorm activity

The sources of electromagnetic energy and electrical behavior of the ambient medium are controlled by the space weather changes such as solar-flares and sun-spots affect the occurrences and characteristics of thunderstorms, the cosmic-ray-produced ions affect the nucleation and growth characteristics of cloud particles. Solar variability moderates the Earth’s electric potential of the ionosphere which is maintained by the world thunderstorm activity. Such a link supports the mechanism in which solar control of ionizing radiation modulates atmospheric electrification, cloud physical processes and atmospheric energetics. On the other hand, the lightning activity in thunderstorms influence the temperature, ion densities, composition and electrical potential of the ionosphere. Recent observations of optical phenomenon such as sprites, elves, blue jets and blue starters propagating from the top of active thunderstorms generate radiations in the ULF and VLF range and contribute to the maintenance of potential of the ionosphere in the global electric circuit (GEC). Horizontal currents flow freely along the highly conducting Earth’s surface and in the ionosphere. GEC is closed by the current flowing from the ground in to the thunderstorm generator and from thunderstorm cloud top towards the ionosphere. There are temporal variations on time-scales varying from microseconds (lightning discharges) to milliseconds (sprites), minutes to an hour (thunderstorm regenerator), hour to a day (diurnal variations), and months (seasonal variations) and to a decade (solar cycle effect). Sprites could change chemically the concentration of HO_x and NO_x in the mesosphere and lower atmosphere. The variable solar activity also affects the weather and climate, thus leading a connection between electrical behavior of the medium and weather and climate.

c. LEP events

Class of transient and localized disturbances of the nighttime lower ionosphere (<100 km altitudes) may occur in association with lightning discharges in at least two different ways: (i) due to the precipitation of bursts of energetic radiation belt electrons by whistler waves injected into the magnetosphere by lightning discharges, and (ii) due to the direct interaction with the collisional lower ionospheric plasma of intense electromagnetic (EM) pulses from lightning.

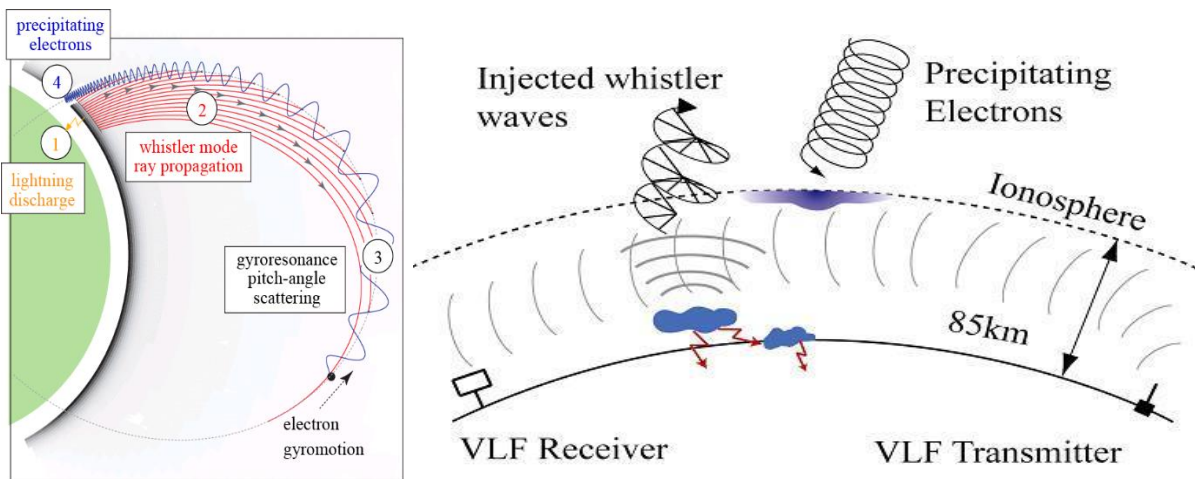


Fig. 3. VLF remote sensing. Left panel shows how whistler modes propagate in the magnetospheric cold plasma, where they interact with trapped electrons. These electrons can be scattered so that they are no longer trapped, but precipitate on to the ionosphere, thereby disturbing. This disturbance in turn affects the propagation of VLF signals from transmitters to receiver paths

One effect, commonly referred to as Lightning-Induced Electron Precipitation (LEP), occurs as a result of the coupling into the Earth's magnetosphere of a relatively small portion of the EM energy from lightning. The wave energy propagates in the whistler-mode between hemispheres in ducts of enhanced ionization and interacts in cyclotron resonance with energetic electrons trapped in the Earth's radiation belts. One result of this interaction is the pitch angle scattering of the electrons and their precipitation into the ionosphere. With typical energies at mid-latitudes of > 50 keV, the short (< 1 s) bursts of precipitating electrons are deposited in the lower ionosphere at altitudes < 100 km, creating secondary ionization, x-rays and heat. The second effect, referred to as Lightning-Induced Heating and Ionization, results from the direct electrodynamic coupling of the intense EM pulse itself with the collisional lower ionospheric plasma. The free electrons of the nighttime D region are accelerated to energies of several eV during the passage of the lightning EM pulse, leading to the generation of optical emissions and impact ionization of the neutrals.

d. Early VLF events

The experimental evidence for the direct upward coupling of lightning energy to the lower ionosphere was also in the form of VLF perturbations observed in association with lightning. However, as opposed to LEP events the onsets of which generally occurred 0.3 to 1.0 s after the causative lightning, these perturbations occurred within <50 ms of lightning or radio atmospherics. The lack of a delay and the rapid onsets of these events were respectively recognized by referring to them as early and fast VLF perturbations. Observation of lower ionospheric heating by VLF transmitter signals suggested that the early/fast VLF perturbations result from the intense heating of the lower ionospheric plasma by the EM radiation from lightning. Although the elevated

electron temperatures exist only as long as the EM pulse from lightning (i.e., 50–100 μ s), sufficient extra ionization is produced to cause all of the observed features of the early/fast subionospheric VLF signals.

e. Solar flares

It was the comparative stability of the amplitude and phase of VLF radio waves that led to the development of VLF transmitters for global navigation and communication. The very existence of navigation systems testifies to the long-term stability of VLF propagation and hence also to the long-term stability of the D-region of the ionosphere, where the VLF waves are reflected. However, VLF wave propagation is directly affected by large scale, transient disturbances such as solar flares and polar cap absorption events. These have been extensively studied via their effects on VLF propagation.

f. Earthquake electromagnetic signatures

Earthquakes are the explosions inside the Earth due to movement and interaction of tectonic plates, which can be characterized by the location of epicenter as well as the main parameters of the rupture (magnitude, seismic moment, source mechanism, orientation of the fault plane and direction of motion). Apart from mechanical properties, there is ample evidence to show the ionospheric perturbations are caused by Earthquakes. Even the electromagnetic emissions (ULF, ELF, VLF and HF ranges) emitted during earthquakes modify the ionosphere while propagating through it. Perturbations in VLF phase and amplitude have been reported to occur before large earthquakes were associated with phase and amplitude variations. The terminator time (TT), is defined as the time where a minimum occurs in the received phase (or amplitude) during sunrise and sunset. A few days before the earthquake the evening TT deviated significantly from the monthly average. Simple theory suggested that the observed effect could be explained by decreasing the VLF reflection height by up to few kms.

g. Cosmic gamma-ray bursts

VLF remote sensing is a sensitive means for probing the lower ionosphere (~40 to 90 km altitude), used to measure celestial X-ray flares which might be monitored by observing annual phase variations on long VLF paths. G.J. Fishman and U.S. Inan [1988] were the firsts to report a transient ionospheric disturbance from a gamma-ray burst, GB830801 which was one of the strongest bursts ever recorded up to that time. The observation path was from GBR (16 kHz) in England to Palmer Station in Antarctica. The more recent, and more spectacular, transient perturbation of VLF propagation created by a gamma-ray flare originated from a magnetar being compact highly magnetized neutron star with the surface magnetic field $\sim 10^{16}$ Gauss, known as a Soft Gamma Repeater (SGR). Transient amplitude changes of more than 20 dB and phase changes of $\sim 65^\circ$ were observed on the path from NPM in Hawaii to Palmer Station in Antarctica. A gigantic periodic flare from the soft gamma repeater SGR 1900+14 produced enhanced ionization at ionospheric altitudes of 30 to 90 km, which was observed as unusually large amplitude and phase changes of very low frequency (VLF) signals propagating in the Earth-ionosphere waveguide. The VLF signals remained perturbed for ~ 5 min and exhibited the 5.16 s periodicity of the giant flare detected on the Ulysses spacecraft. Quantitative analysis indicates the presence of an intense initial low energy (3–10 keV) photon component that was not detectable by the Ulysses instrument.

II. Ionospheric study in F-layer using GPS stations located in Tashkent and Kitab

Electromagnetic wave signals are perturbed when travelling through the ionosphere. As the ionosphere is a dispersive medium, the ionospheric refraction depends on the signal frequency. The effect of ionospheric refraction is to delay signal propagation. This causes a delay and advance for the GPS code and phase measurements.

TEC extraction

One of the most important characteristics of the Earth's ionosphere is the total electron content (TEC), however, to date, over the territory of Central Asia its global monitoring was not performed. Analytical models give a good estimate of this parameter provided quiet geomagnetic conditions, but in the case of a perturbed ionosphere TEC assessment becomes less accurate.

Radio-raying of the atmosphere by means of signals of satellite navigation systems and a network of ground stations are readily available and low-cost way to monitor the F-layer of the ionosphere in real time. On the basis of this technique, it is created software to analyze GPS data in the Receiver Independent Exchange (RINEX) format, provided an international network of the International GNSS Service (IGS).

Total Electron Content

TEC is a frequently used quantity in ionospheric science. Since the number of electrons approximately equals to the number of positive ions, the TEC represents a suitable parameter for the degree of ionization. The TEC is defined as the integral over the electron density distribution N_e along a defined path s :

$$TEC = \int N_e ds. \quad (1)$$

Since N_e is a volumetric density and TEC is defined by the integral over a path, the TEC can be thought as the total number of electrons that is contained in a volume with a cross section area being equal to 1 m^2 and length being equal to the path length. The common unit used for measuring the TEC is called Total Electron Content unit (TECU) and 1 TECU is equivalent to 10^{16} el/m^2 . Depending on local time, Solar activity, geomagnetic conditions, region of the Earth, etc., the vTEC can vary from about 1 to 180 TECU.

Method of data analysis

Space segment of GPS (Global Positioning System) nominally consists of 24 main satellites and four spares. Spacecrafts are moving along six circular orbits at 20200 km with the inclination angle 55° and evenly spaced in the longitude by 60° . This configuration assumes that at any point on the Earth at any time in the zone of radio visibility there are 6-8 satellites which allow the continuous monitoring of the ionosphere. Each GPS satellite emits two high-stable signals at the frequencies $f_1 = 1575.42 \text{ MHz}$ and $f_2 = 1227.60 \text{ MHz}$. The signals are refracted due to electron density gradients, and since the ionosphere is a dispersive medium, the ray paths of the f_1 and f_2 signals will be slightly different. The obtained phase and pseudorange measurements contain information about the TEC along the ray paths. Dual-frequency group delay measurements of signals of GPS satellites can provide ionospheric delay of the signal, and accordingly determine the absolute value of TEC, which is proportional to this delay.

GPS technology is realized simultaneously measuring the group (P1, P2) and phase (L1, L2) delay signals f_1 and f_2 , which can be written as follows, see e.g.:

$$P_i = \rho + c(dt^{rec} - dt^{sat}) + \Delta_i^{iono} + \Delta^{tropo} + \Delta^{instr}, \quad (2)$$

$$L_i = \rho + c(dt^{rec} - dt^{sat}) - \Delta_i^{iono} + \Delta^{tropo} + \Delta^{instr} + \lambda_i N_i, \quad (3)$$

where the index $i=1;2$ corresponds to the carrier frequencies f_1 and f_2 ; P is the code pseudorange measurement (in distance units); ρ is the geometrical range between satellite and receiver; c is the vacuum light speed; dt^{rec} and dt^{sat} are the receiver and satellites clock offsets from GPS time; $\Delta_i^{iono} = 40.3 \cdot TEC / f_i^2$ is the ionospheric delay; TEC is the Total Electron Content; Δ^{tropo} is the tropospheric delay; Δ^{instr} is the receiver and satellite instrumental delay; L_i is the carrier phase observation (in distance units); λ_i is the wavelength; N_i is the unknown integer carrier phase ambiguities.

Combining the pseudoranges observations P_i , a TEC value is obtained as

$$TEC_p = 9.52 \cdot (P_2 - P_1), \quad (4)$$

which is very noisy and after combination of carrier phase observations L_i one can get

$$TEC_L = 9.52 \cdot [(L_1 - L_2) - (\lambda_1 N_1 - \lambda_2 N_2)], \quad (5)$$

which is less noisy than TECP, but it is ambiguous. In practice, the calculation of TEC using the pseudorange data only can produce a noisy result. It is desirable to use in addition the relative phase delay between the two carrier frequencies in order to obtain a more precise result. Differential carrier phase provides a precise measurement of relative TEC variations. However, the absolute TEC cannot be found unless the pseudorange is also used because the actual number of cycles of phase is unknown. Pseudorange gives the absolute scale for the TEC while the differential phase increases measurement precision.

The process of extracting data from RINEX files has been done by using Matlab programming language whereby the RINEX file was obtained from the GPS receiver. The script in Matlab program software analyzes and extracts the information needed in calculating the TEC from the observation and navigation RINEX files. The results of the calculation can be shown as the graphs of elevation angle, different phase, different delay, Slant TEC (STEC) and Vertical TEC (VTEC) versus time. The data of VTEC can be used as the absolute quantity since its value does not depend on the location of satellite receiver compared to STEC.

GIS and Remote Sensing technologies for digital mapping

GIS technologies provide a good platform for modelling by collecting and storing, managing, analyzing and displaying data. Remote sensing technology is used to provide information on land use using digital imaging techniques [Yüksel *et al.*, 2008].

Images obtained from the Landsat satellite are widely used in natural resource mapping and monitoring studies worldwide. Images of the ASTER satellite are also in demand for the Central Asia region. With ASTER DEM, you can obtain a digital relief model that is very useful for mountain areas. The spatial resolutions of Landsat and ASTER satellites are the same and equal to 30 m. These satellite data are very useful for areas where there is a data shortage.

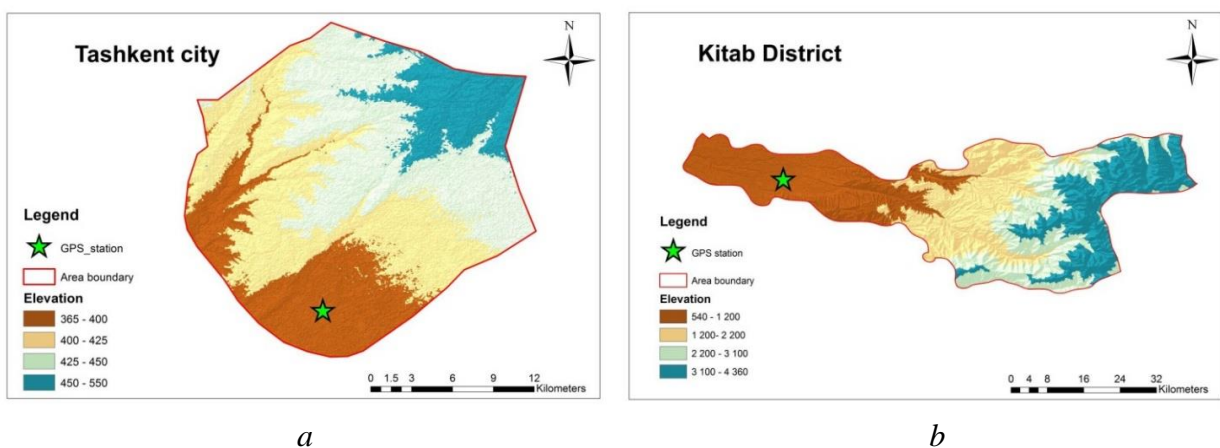


Fig. 4. a) GPS stations location maps in Tashkent city
b) GPS stations location maps in Kitab district

A GPS stations location maps in Tashkent city and Kitab district (fig. 4 a, b) were produced using ArcGIS 10.3 desktop software [Mirzaev *et al.*, 2019]. A WGS84 geographic coordinate system was used as a reference datum. Advanced Spaceborne Thermal Emission and Reflection

Radiometer Digital Elevation Model¹ was utilized to prepare the elevation map. Using open source datasets is a way to upgrade remote sensing and GIS skills, especially for researchers in developing countries. Landsat optical satellite images and ASTER DEM are frequently used for different research areas [Lu et al., 2004].

Slant and Vertical TEC

Slant TEC is a measure of the total electron content of the ionosphere along the ray path from the satellite to the receiver, represented in fig. 5 as the quantity STEC. It can be calculated by using pseudorange and carrier phase measurements as described above. As STEC is a quantity which is dependent on the ray path geometry through the ionosphere, it is desirable to calculate an equivalent vertical value of TEC which is independent of the elevation of the ray path. The STEC is expressed in Total Electron Content Units (TECU): $TECU=10^{16}$ electrons per m^2 .

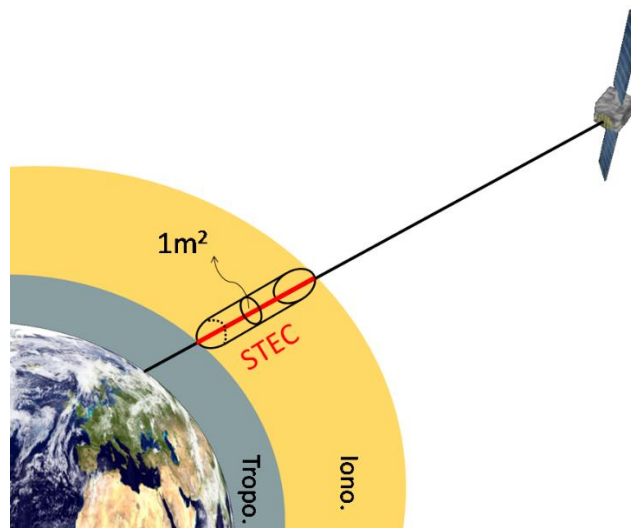


Fig. 5. Slant Total Electron Content in F-layer of the ionosphere

In order to refer the resulting VTEC to a point with specific coordinates, i.e. in order to assign the VTEC value to a specific point in the ionosphere, the so-called single-layer (or thin-shell) model is usually adopted for the ionosphere.

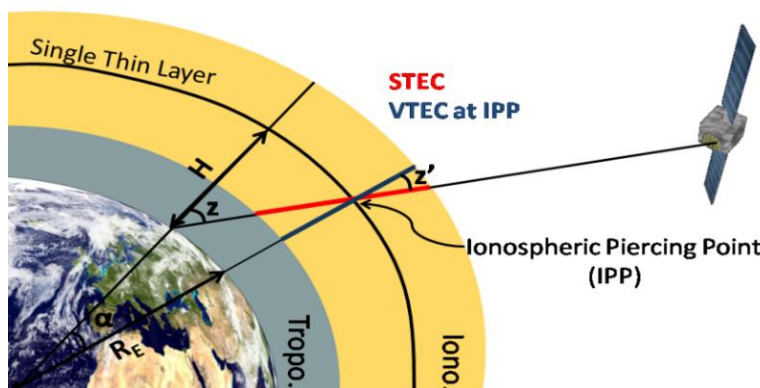


Fig. 6. STEC versus VTEC in F-layer of the ionosphere

¹ASTER DEM. Advanced Spaceborne Thermal Emission and Reflection Radiometer, Digital Elevation Model. 2019.

Fig. 6 shows a schematic representation of this model. In this model all free electrons are contained in a shell of infinitesimal thickness at altitude H . This idealized layer is usually set to be at 350, 400 or 450 km, approximately corresponding to the altitude of maximum electron density. Fig. 5 depicts the relationship between Slant (STEC) and Vertical (VTEC) TEC.

VTEC can be regarded as:

$$VTEC = STEC \cdot \cos z', \tag{6}$$

with

$$\sin z' = \frac{R_E}{R_E + H} \sin z \tag{7}$$

Here R_E is the mean Earth radius of 6371 km, H is the maximum height of the electron density.

RESULTS OF RESEARCHES AND THEIR DISCUSSION

We have analyzed several earthquakes (EQs) occurred with magnitude $M > 5.0$ for which the transmitter–receiver signal path was more closed to the epicenter and crossed the EQ preparation zone circle. The amplitude data are analyzed here due to the fact that the perturbations in the amplitude data are clearly identified than that in the phase data. We have observed significant changes in amplitude parameters (trend, N.F., D and their normalized values). The results obtained show principal possibility to detect the EQ precursors before the occurrence of EQ.

We are continuously monitoring the D-Layer of the ionosphere to study ionospheric disturbances starting June, 2008. Several EQ events are registered by Tashkent VLF receiver and being analyzed. We have observed significant changes in amplitude parameters (trend, NF, D and their norms), a few days before the strong EQs occurred on the path way from the transmitters to Tashkent VLF receiver. The mean nighttime amplitude (or trend) and normalized trend are found to increase significantly before the EQs with the same tendency as the NF and normalized NF. In general, the anomalies occurred 0–13 days before the strong EQs are identified as ionospheric EQ precursors. The obtained results are in good agreement with the previous observations of EQs precursors in VLF data reported by various researchers [Hayakawa, Fujinawa, 1994; Pulinets, Boyarchuk, 2004].

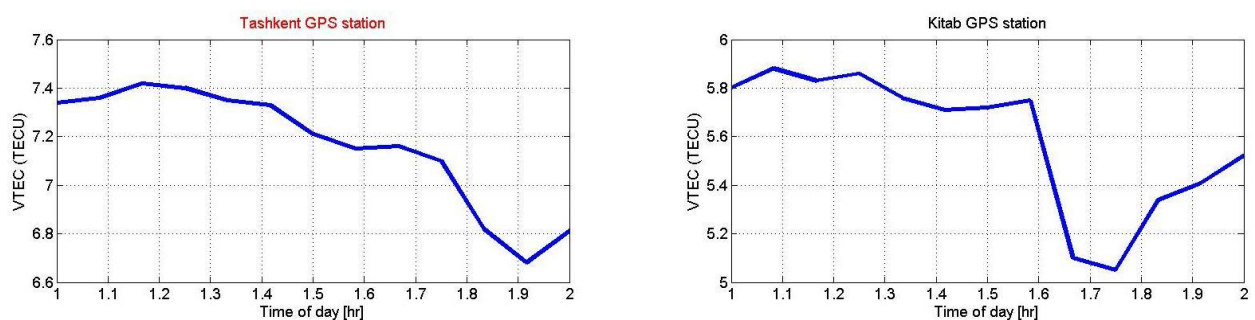


Fig. 6. TEC at KIT3 and TASH stations 1:00–2:00 h UTC

Table 1. List of 2 GPS stations, location, mean TEC and range error

N _o	Station ID	Latitude	Longitude	Mean TEC Value (TECU)	Range Error (Meter)
1	KIT3	39.1348	66.8854	5.4444	0.8711
2	TASH	41.1933	69.1776	7.1368	1.141888

The data analysis on X-ray Solar Flares and Total Solar Eclipse are introduced in order to justify that the Tashkent VLF receiver is properly functioning and can detect the ionospheric disturbances in the correct way. Few solar flare events are observed by VLF signals during 2010 and 2011 and the analysis showed that there is simultaneous correlation between the time of change of amplitude of the waves and the Solar Flares. A Solar Eclipse is observed on 22 July 2009 on the path ways of VLF signals from JJI (Japan), NWC (Australia) and VTX (India) transmitters.

The location of two GPS stations are used in this research as illustrated in table 1. Fig. 6 shows TEC for Kitab and Tashkent GPS stations during one hour. The mean TEC values extracted from the data at these stations are calculated and presented in the table 1. From this value, positioning error can be estimated based on $1 \text{ TECU} = 0.16 \text{ m}$ range error. Fig. 6 shows the Vertical TEC at Kitab (KIT3) and Tashkent (TASH) stations during 1 h UTC. The analysis at an equatorial region used SLM mapping function where the peak altitude ranges from 350, 400 or 450 km. The resulted vertical TEC are precise, accurate and without multipath, unless the multipath environment is really terrible, in which case a small, residual amount of multipath can even be seen in the differential carrier phase. The calculated range errors observed were from 0.8711 m to 1.141888 m at different receiver locations.

We have studied the TEC value for Uzbekistan regions, based on analysis of continuous data from the Tashkent and Kitab GPS stations. The leveling process is used in dual-frequency GPS signal to calculate TEC and to estimate positioning error from this value. Single Layer Model (SLM) model is used to convert Slant TEC (STEC) to Vertical TEC (VTEC) as shown in fig. 3. Tashkent and Kitab GPS stations have geographic latitudes $41^{\circ}19'33''\text{N}$, $39^{\circ}13'48''\text{N}$, longitudes $69^{\circ}17'76''\text{E}$, $66^{\circ}88'54''$, respectively, and the positioning errors are ranging from 0.8711 m to 1.141888 m with respect to the receiver locations i.e. it has shown encouraging results based on the utilization of carrier phase observation for precise positioning.

CONCLUSIONS

The empirical formulae as a function of elevation angle and TEC have been developed for the differential GPS stations that can be used for any location over equatorial region. Since this model is independent of azimuth, baseline length and orientation, it has the potential to improve the single frequency method over the network solution.

Thus, there are several methods to make a prediction including ones based on GPS TEC measurements. The simultaneous permanent monitoring of F-layer using GPS devices (operating in Tashkent and Kitab) indicates the observable TEC variation before the local EQs. As an alternative method for plausible prediction of seismic disturbances in the ionosphere might be the use of combined ground and satellite-based observations.

ACKNOWLEDGEMENTS

This research is supported by grants No VA-FA-F-2-008, No MRB-AN-2019-29 and No YFA-Ftech-2018-8 of the Uzbekistan Ministry for Innovative Development, by the Abdus Salam International Centre for Theoretical Physics through Grant No OEA-NT-01 and by an Erasmus+ exchange grant between SU and NUUZ. Author would like to thank Sardor Tojiev and Yusufjon Tillayev for their invaluable help, fruitful discussions and programming on the ways of TEC extraction from the GPS data.

REFERENCES

1. *Fishman G.J., Inan U.S.* Observation of an ionospheric disturbance caused by a gamma-ray burst. *Nature*, 1988. V. 331. P. 418–420. DOI: 10.1038/331418a0.
2. *Hayakawa M., Fujinawa Y.* Electromagnetic phenomena related to earthquake prediction. Tokyo: Terra Scientific Publishing, 1994. 677 p.
3. *Lu D., Mausel P., Brondizio E., Moran E.* Change detection techniques. *International Journal of Remote Sensing*, 2004. V. 25. No 12. P. 2365–2407. DOI: 10.1080/0143116031000139863.

4. *Mirzaev B., Mamatov F., Tursunov O.* A justification of broach-plow's parameters of the ridge-stepped ploughing. *E3S Web of Conferences*, 2019. V. 97. DOI: 10.1051/e3sconf/20199705035.
 5. *Pulinets S., Boyarchuk K.* Ionospheric precursors of earthquakes. Berlin: Springer Science & Business Media, 2004. 316 p.
 6. *Rishbeth H., Garriott O.K.* Introduction to ionospheric physics. International geophysics series. New York and London: Academic Press, 1969. V. 14. 344 p.
 7. *Tojiev S.R., Ahmedov B.J., Eshkuvatov H.E.* Ionospheric precursors of earthquakes recorded by VLF receiver at Tashkent IHY station. *Advances in Space Research*, 2014. V. 54. P. 628–643. DOI:10.1016/j.asr.2014.04.027.
 8. *Yüksel A., Akay A., Gundogan R.* Using ASTER imagery in land use/cover classification of eastern mediterranean landscapes according to CORINE Land Cover Project. *Sensors*, 2008. V. 8. P. 1237–1251. DOI: 10.3390/s8021287.
-